MACEIÓ - ALAGOAS
EBA 15
15° ENCONTRO BRASILEIRO SOBRE ADSORÇÃO
15th Brazilian Meeting about Adsorption

Fixed-bed adsorption of Escitalopram onto a niobium-based nanozeolite

Leandro Rodrigues Oviedo[a], Daniel Moro Druzian[b], Sthéfany Nunes Loureiro[c], Lissandro Dorneles Dalla Nora[d], William Leonardo Da Silva[e*]

[a]*Franciscan University (UFN), Email: leandro.roviedo@gmail.com, Santa Maria-RS ZIP:97010491, Brazil*
[b]*Franciscan University (UFN), Email:daniel.druzian@ufn.edu.br, Santa Maria-RS ZIP:97010491, Brazil*
[c]*Franciscan University (UFN), Email:s.loureiro@ufn.edu.br, Santa Maria-RS ZIP:97010491, Brazil*
[d]*Franciscan University (UFN), Email:lissandro@ufn.edu.br, Santa Maria-RS ZIP:97010491, Brazil*
[e]*Franciscan University (UFN), Email:w.silva@ufn.edu.br, Santa Maria-RS ZIP:97010491, Brazil*

Abstract

Drugs (e.g., Escitalopram) are challenging to remove from water due to their chemical/thermal stability, low biodegradability and resistance to conventional water treatments. Nanozeolites have been attracted to the adsorption field due to their high surface area, thermal stability, and acidity. Nanozeolite acidity can be enhanced by the incorporation of metals/semi-metals in its structure. Thus, the present work aims to synthesize and characterize a niobium-based zeolitic nanoadsorbent for the removal of the Escitalopram drug from water, in a fixed-bed operation. Niobium-based nanozeolite (nFAU@10_Nb) was obtained by hydrothermal method combining zeolite precursors and ammonium niobium(V) oxalate (10 wt.%), followed by calcination at 500°C for 120 min. The nFAU@10-Nb was characterized by XRD, DLS, and pH_{ZCP}. XRD identified faujasite, niobium pentoxide, and lueshite for nFAU@10_Nb and ZP = -5.05 ± 2.25 mV. nFAU and nFAU@10_Nb showed pH_{ZCP} 7.06 and 6.72, respectively. The fixed-bed adsorption showed 80% drug removal up to breakthrough time (35 min) for nFAU, whereas 89% removal was reported up to 50 min under 20 mL min^{-1}, pH 7.71, and 1.0 g of nanoadsorbent. The experimental data were better fitted by Thomas model, indicating a high affinity between the Escitalopram and the nanoadsorbent. nFAU@10_Nb showed higher column adsorption capacity (q_e = 3.39 mg g^{-1}) than nFAU (q_e = 0.87 mg g^{-1}). The maximum adsorption capacity for nFAU and nFAU@10_Nb were 81.8 and 74.6 mg g^{-1}, respectively. Therefore, this work confirms that niobium can enhance the adsorption capacity and acidity of alternative nanozeolites, being useful as a starting point for scale-up studies.

Keywords: Niobium; Nanozeolites; Drugs; Nanoadsorbents; Sustainability

1. Introduction

Since the onset of the COVID-19 pandemic in 2019, there has been a noticeable rise in the consumption of psychiatric drugs, such as antidepressants, anti-anxiety drugs, mood stabilizers, and antipsychotics [1].

These contaminants are particularly challenging to eliminate due to their chemical and thermal stability, low biodegradability, and high water solubility, which make them resistant to conventional wastewater treatment methods [2]. In addition, pharmaceutical residues can accumulate in aquatic organisms, leading to endocrine disruptions and various health issues such as reproductive, developmental, and metabolic disorders [3].

Nanozeolites have emerged as a promising solution for environmental remediation. With their acidity, higher surface area, pore volume, and stability compared to micro-sized zeolites, nanozeolites exhibit a strong affinity for organic pollutants [4]. In addition, nanozeolites can be synthesized through eco-friendly methods using residual alumina and silica [5]. Moreover, the nanozeolites' acidity can be enhanced with the incorporation of some elements in its chemical composition, such as zirconium (Zr), lanthanum (La), zinc (Zn), niobium (Nb), aluminum (Al) and boron (B) [6]. These chemical changes can significantly enhance the Lewis acidity and hence, lead to a higher affinity of nanozeolite for organic pollutants, including pharmaceutical contaminants [7]. In this view, the present work aims to synthesize and characterize a niobium-based zeolitic

nanoadsorbent for the removal of the Escitalopram drug from an aqueous solution, in a fixed-bed operation.

2. Materials and Methods

2.1. Synthesis of Zeolite, and Zeolite with Nb

The Faujasite nanozeolite (nFAU) was synthesized by hydrothermal using the (agro)industrial waste such as rice husk (grain processing industry), and residual sludge (water treatment plant). In this sense, 2.15 g of Al_2O_3 and 0.68 g of SiO_2 were diluted in 60 mL of 2 mol L^{-1} NaOH (99%, Synth®) under magnetic stirring (150 rpm / 25 ± 2 °C for 20 min). Subsequently, the mixture was transferred to a reaction in a stainless-steel autoclave lined with polytetrafluoroethylene (PTFE) heated at 90 °C for 600 min, washed, and dried in an oven at 80 °C for 720 min [8]. Furthermore, the same procedure was repeated with the addition of 10% (m/m) of Ammonium niobate(V) oxalate hydrate ($C_4H_4NNbO_9 \cdot H_2O$, 99%, Sigma-Aldrich®). Then, the final material was calcinated at 500°C for 120 min at a 10 °C min^{-1} rate.

2.2. Characterization of Zeolites

The crystalline phases of the samples were identified by X-ray Diffraction (XRD) in a Bruker diffractometer (model D2 Advance) using a copper tube ($\lambda_{Cu-\alpha}$ = 0.15406 nm, Bragg angle ranging from 5° to 70°, and accelerating voltage and current of 30 kV and 30 mA, respectively. Moreover, the Bragg and Debye-Scherrer equations were used to determine the interplanar distance (d) and the average crystallite size (d_c), respectively, specified in Equation (1)-(2) [9]. The surface charge of the zeolites (zeta potential) was determined by Doppler Light Scattering in the Malvern-Zetasizer® equipment (model nano ZS, ZEN3600). The characteristics in an aqueous medium such as Hydrodynamic Particle Diameter (PHd) and Polydispersity (Pd) of the samples were established by Dynamic Light Scattering (DLS). The zero charge point (pH_{ZCP}) of the samples was determined using the 11-point test calculating the ΔpH [10].

$$d = \frac{n * \lambda_{Cu-\alpha}}{2 * sen\ (\theta)} \quad (1)$$

$$d_c = \frac{0.94\ * \lambda_{Cu-\alpha}}{\beta * cos\ (\theta)} \quad (2)$$

Where: θ = Bragg diffraction angle (°); n is the diffraction order; and β = full width at half maximum (FWHM).

2.3. Adsorption of Escitalopram in Fixed-bed Column

The fixed-bed adsorption was carried out on a bench-scale system (20 L) operating at flow rate 20 mL min^{-1}, adsorbent mass 1.0 g and at pH 4 and 8. The absorbance of the effluent was measured in a UV-Vis Spectrophotometer (Shimadzu) at a wavelength equal to 239 nm (maximum light absorption of Escitalopram), with the aliquots (3 mL) collected at predetermined intervals (0, 3, 5, 10, 15, 30, 45, 60, 75, 90, and 120 min). The experimental data were fitted to the Thomas, and Yoon-Nelson non-linear kinetic models [11].

3. Results and Discussion

3.1. Characterization Results of Zeolites

The Figure 1(a) presents the XRD patterns of the samples, where the nFAU@10_Nb presented the crystalline phases: Faujasite ($AlNaO_{5.4}Si_{1.7}$, JCPDS n° 12-0228, d_c= 14.55 nm) at 6.21° (111, d= 7.09 Å), 10.06° (220, d= 4.39 Å), 11.88° (221, d= 3.72 Å), 15.68° (222, d= 2.83 Å), 20.19° (440, d= 2.22 Å), 23.02° (553, d= 1.95 Å), and 31.13° (555, d= 1.48 Å); Niobium Pentoxide (Nb_2O_5, JCPDS n° 43-1042, d_c= 21.72 nm) at 14.01° (012, d= 3.16 Å), 24.44° (110, d= 1.85 Å), 26.72° (111, d= 1.70 Å), 32.60° (312, d= 1.42 Å), and 50.22° (221, d= 1.00 Å); and Lueshite ($NaNbO_3$, JCDPS n° 75-2102, d_c= 42.87 nm) at 22.82° (001, d= 1.97 Å), 46.67° (002, d= 1.05 Å), 52.50° (380, d= 0.96 Å), and 57.97° (212, d= 0.90 Å) confirming the presence of Nb in the nanostructure of the Faujasite nanozeolite. Furthermore, the formation of the Lueshite phase is due to the amount of sodium used to solubilize the components. Table 1 shows the surface properties of the Samples.

Table 1. Surface properties of samples.

Samples	ZP (mV)	PHd (nm)	Pd
nFAU	-16.1 ± 2.76	3522 ± 788	0.58 ± 0.05
nFAU@10_Nb	-5.05 ± 2.25	1222 ± 181	0.67 ± 0.07
Escitalopram	-12.4 ± 1.77	381 ± 87	0.32 ± 0.04

According to Table 1, the nFAU presented a negative surface charge indicating electrostatic repulsion with the escitalopram. However, the pH_{ZCP} demonstrated in Figure 1(b) of nFAU@10_Nb was of 6.72 indicating a protonated surface in adsorbent when the pH was above the pH_{ZCP} causing an increase in electrostatic interactions and adsorption. Moreover, the HPz (>1000 nm), and Pd (>0.6) values of the zeolites indicated an overestimated value due to the strong electrostatic interactions between the solvent and the constituents generally oxides of silicon, aluminum, sodium, and niobium. In this sense, the stability of the zeolites can be explained due to the tendency of the atoms to relax, reducing the surface energy and agglomerating the particles [12].

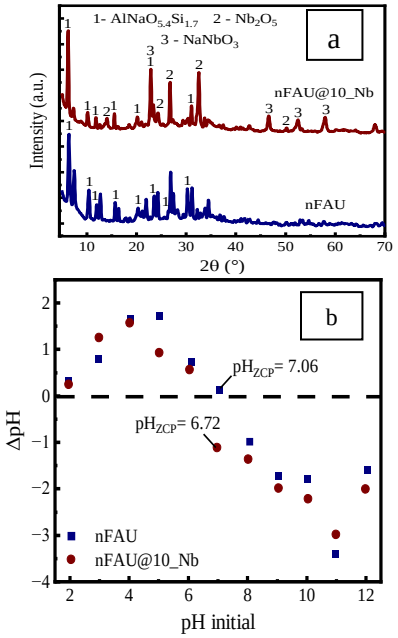

Figure 1. (a) Diffractograms; and (b) pH_{ZCP} of Zeolites

3.2. Adsorption

Table 2 shows the results of the adsorption column performance for all samples based on the breaktrhough time (t_r), the fraction of the bed used for adsorption ($F_{bed,ads}$) and adsorption capacity (q_e)

Table 2. Fixed-bed adsorption performance of the samples and the column adsorption capacity

Samples	pH	t_b (min)*	$F_{bed,ads}$ (%)	q_e (mg g^{-1})
nFAU	8	35	63.6	0.87
nFAU@10_Nb	8	50	65.9	3.39
nFAU@10_Nb	4	44	70.9	2.63

* time at which C/Co = 0.20 | 25°C | adsorbent mass = 1.0 g | bed height = 1.5 cm

According to the results, t_b was higher for nFAU@10_Nb than the pristine nFAU, which indicates that more adsorption of Escitalopram occurs during the fixed-bed operation. According to experimental results, around 80% adsorption is reported for nFAU at 35 min, whereas 88-89% is observed for nFAU@10_Nb at 44 and 50 min. Moreover, Escitalopram shows pKa 9.8, which indicates that the amine groups are fully protonated, which enhances the electrostatic interaction of this drug with the negative surface of nFAU at pH 8. Furthermore, the incorporation of Nb in the nFAU increased its adsorption capacity and acidity[14]. It was probably due to the enhanced Lewis acidity of the nanozeolite by the presence of Nb and some Al in the nanoadsorbent structure [15]. Moreover, the acidic Lewis sites of nFAU@10_Nb attributed to the Nb and Al atoms can promote higher interactions between F and N atoms present in the chemical structure of Escitalopram. Moreover, this result can be attributed to the Nb-based precursor (ammonium niobate(V) oxalate) used in the nanozeolite synthesis, which can act as a porogenic agent, generating mesoporosity in the nanoadsorbent [16].

3.3 Kinetic studies

The adsorption data were fitted to Thomas and Yoon-Nelson kinetic models. The results of curve fitting are shown in Table 3.

Table 3. Curve fitting of experimental data

	Thomas	
	nFAU	nFAU@10_Nb
k_{TH} (L mg^{-1} min^{-1})	0.038	0.035
q_{max} (mg g^{-1})	95.10	81.77
R^2	0.9972	0.9780
	Yoon-Nelson	
K_{YN} (min^{-1})	0.076	0.9954
τ (min)	51.82	74.60
R^2	0.9971	0.9783

* Flow rate = 20 mLmin^{-1}| adsorbent mass = 1.0 g | pH 8

According to Table 3, the adsorption of Escitalopram onto nFAU data was better fitted by the Thomas model, indicating that the adsorption

process may be governed by a more balanced dynamic between adsorption and desorption, suggesting a more uniform distribution of active sites on the nFAU@10_Nb surface [17]. However, regarding the adsorption of Escitalopram on nFAU@10_Nb, the Yoon-Nelson model was reported as the best fit, indicating a high affinity between the Escitalopram and the nFAU surface, resulting in efficient occupation of adsorption sites [18]. According to the Thomas model, the maximum adsorption capacity for nFAU and mFAU@10_Nb were 81.8 mg g^{-1} and 74.6 mg g^{-1}, respectively

4. Conclusion

A novel nanoadsorbent was successfully synthesized in two steps. The incorporation of niobium by the use of oxalate-based precursor resulted in a higher adsorption capacity for faujasite. Therefore, this strategy was suitable for producing nanozeolites with enhanced performance in fixed-bed adsorption. Furthermore, future studies involving variations in fixed-bed diameter, bed height and flow rate are required to obtain more information on the process. Therefore, the findings reported in this work can be used as a starting point for scale-up studies.

Acknowledgements

The authors would like to thank GPNAp and UFN) for their support/assistance in carrying out the present work. This study was financed in part by the Coordenação de Aperfeiçoamento de Pessoal de Nível Superior Brasil (CAPES) - Finance Code 001.

References

[1] Jacob L, Bohlken J, Kostev K. Increased pharmacy purchases of cardiovascular drugs from wholesalers prior to the first and second COVID-19 lockdowns. J Psychiatr Res 2021; 140:346-349.

[2] Teymoorian T, Teymourian T, Kowsari E, Ramakrishna S. A review of emerging PFAS contaminants: sources, fate, health risks, and a comprehensive assortment of recent sorbents for PFAS treatment by evaluating their mechanism. J Water Proc engineering 2021; 42:102193-102216.

[3] Kayode-Afolayan SD, Ahuekwe EF, Nwinyi OC. Impacts of pharmaceutical effluents on aquatic ecosystems. Sci Afr 2022;17:e01288-e01290.

[4] Shojaei S, Nouri A, Baharinikoo, Farahani MD, Shojaei S. Removal of the hazardous dyes through adsorption over nanozeolite-X: Simultaneous model, design and analysis of experiments. Polyhedron 2021;196:114995-115115.

[5] Yoldi M, Fuentes-Ordoñez E, Korili S, Gil A. Zeolite synthesis from industrial wastes. Micropor Mesopor Mat 2019;287:183-191.

[6] Gehring B, Traa Y, Hunher M. Elucidation of the versatile Brønsted acidity of nanosized ZSM-5 materials. Micropor Mesopor Mater 2021;317:110978-110986.

[7] Zhang HL, Zheng AM, Deng ZW. The Effect of Zirconium Incorporation on the Brønsted Acidity of Zeolite: A DFT Study. Applied Mechanics and Materials 2010;44-474:3616-3619.

[8] Oviedo LR, Druzian DM, Montagner GE, Ruiz YPM, Galembeck A, Pavoski G, Espinosa DCR, Nora LDD, Da Silva WL. Supported heterogeneous catalyst of the copper oxide nanoparticles and nanozeolite for binary dyes mixture degradation: Machine learning and experimental design. J Mol Liq 2024;402:124763-781.

[9] Hulbert BS, Kriven WM. Specimen-displacement correction for powder X-ray diffraction in Debye-Scherrer geometry with a flat area detector. J App Crystallogr 2023;56:160-66.

[10] El-Fadl FIA, Elbarbary AM. Radiation synthesis and characterization of heterogeneous magnetic nanocomposites of 2-hydroxyethyl methacrylate for catalytic degradation of sandocryl blue dye. Sep Purif Technol 2021;272:118972-986.

[11] Hanbali M, Holail H, Hammud H. Remediation of lead by pretreated red algae: adsorption isotherm, kinetic, column modeling and simulation studies. Green Chem Lett Rev Gree 2014;7:342-358.

[12] Aljama HA, Gordon MH, Bell AT. Assessing the stability of Pd-exchanged sites in zeolites with the aid of a high throughput quantum chemistry workflow. Nat Commun 2022;13: 2910-919.

[13] Liu C, Li G, Hensen EJM, Pidko EA. Relationship between acidity and catalytic reactivity of faujasite zeolite: A periodic DFT study. J Catal 2016;344:570-577.

[14] Ferreira C, Araujo A, Calvino-Casilda, Cutrufello MG, Rombi E, Fonseca AM, Bañares MA, Neves IC.Y zeolite-supported niobium pentoxide catalysts for the glycerol acetalization reaction. Micropor Mesopor Mat 2018;271:243-251.

[15] Ziolek M, Nowak I, Karge HG. Solid-state interaction between niobium oxide and Y-type zeolites. Stud Surf Sci Catal 1995;94:270-277.

[16] Lima LFS, Olusegun SJ, Mohallem NDS. Niobium pentoxide/silica nanocomposites with hierarchical pore structure as methylene blue and doxycycline adsorbent. Mater Chem Phys 2023;308:128234.

[17] Zou W, Bai H, Zhao L, Li K, Han R. Characterization and properties of zeolite as adsorbent for removal of uranium(VI) from solution in fixed bed column. J. Radioanal. Nucl. Chem. 2011;288:779-788.

[18] Salihi EC, Tulay EC. Adsorptive removal of antipsychotic drug by carbon nanofibers in a batch and fixed bed column system. Particul Sci Technol 2022;40:889-91.